communications biology

A Nature Portfolio journal

Article

https://doi.org/10.1038/s42003-025-07987-z

# Paclobutrazol induces triterpenoid biosynthesis via downregulation of the negative transcriptional regulator SlMYB in *Sanghuangporus lonicericola*

Check for updates

Dong-Xue Zhang[1,2,3], Bi-Yang Liu[1,2,3], Fei-Fei Xue[1,2,3], Yu-Lin Tang[1,2,3], Meng-Jiao Yan[1,2,3], Si-Xian Wang[1,2,3], Lu Guo[1,2,3], Tian Tong[1,2,3], Li-Nan Wan[1,2], Yong-Nan Liu[1,2,3], Xiao-Ling Wang[1,2,3] ✉ & Gao-Qiang Liu[1,2,3] ✉

Triterpenoids are well-known pharmacological components of *Sanghuangporus* fungi, such as *Sanghuangporus lonicericola*. This study investigates the inductive effects of paclobutrazol (PBZ) on triterpenoid biosynthesis in the submerged fermentation of *S. lonicericola* and explores the induction mechanisms via multi-omics and genetic methods. The addition of 100 mg/L PBZ significantly increases the triterpenoid yield by 151.39%. A total of 29 triterpenoids are tentatively identified, of which 18 are newly presented only under PBZ induction. Moreover, 30 genes involved in the MVA pathway and 31 genes encoding cytochrome P450 monooxygenases assumed to be responsible for decoration are identified. Finally, a MYB transcription factor (SlMYB) is identified and found to be downregulated under paclobutrazol induction. Genetic manipulation of *SlMYB* demonstrates its negative regulatory effect on four putative target genes, including *ACAT*, *MVD*, *IDI*, and *FDPS*. Electrophoretic mobility gel shift assays verify the direct interactions with the promoters of *MVD*, *IDI*, and *FDPS*. Taken together, PBZ acts as an effective inducer of triterpenoid biosynthesis in *S. lonicericola*, and the transcription factor SlMYB is negatively regulated.

Macrofungi are rich and highly diverse bioactive metabolites that are considered a valuable pool of bioresources. "Sanghuang" is a group of macrofungi traditionally used for both medicinal and edible purposes. However, their classifications and *Latin* names are controversial. Researchers used multi-gene fragment alignment analysis to confirm that "Sanghuang" and similar species belong to a new genus and thus established the *Sanghuangporus* genus[1]. *Sanghuangporus lonicericola* is one of the *Sanghuangporus* group that have been identified worldwide[1–5]. *Sanghuangporus* fungi have attracted extensive attention due to their various medicinal ingredients, such as polysaccharides, polyphenols, terpenes, and flavonoids[6,7]. Of these, triterpenoids are the key pharmacologically active compounds responsible for medicinal functions, such as antioxidant[8], antibacterial, and anti-tumor activities[9] in vitro in *Sanghuangporus* species.

Triterpenoids have great potential for commercial use. Therefore, it is crucial to effectively improve their biosynthesis efficiency and production owing to the shortage of wild resources of *Sanghuangporus* basidiocarps in nature. Progress has been achieved in improving secondary metabolite production from different *Sanghuangporus* spp. by manipulating submerged fermentation strategies using chemical inducers. For example, the application of polyunsaturated fatty acids[10], fungal elicitors[11], phytohormones, including methyl jasmonate[12,13], and salicylic acid[14], has been validated to improve the yield of triterpenoids in *Sanghuangporus* fungi. Plant growth regulators (PGRs) can modulate secondary metabolite biosynthesis in plants[15,16]. In this study, PBZ, a PGR, was commonly used to modify the growth, yield, quality, and physiological traits of plants[17]. Notably, the application of PBZ can affect the terpenoid biosynthetic pathway in plants. Quinone methide triterpenes (QTs) were enhanced by the association of gibberellin acid with PBZ in *Monteverdia floribunda*[18]. The composition of lavender oil was altered in relation to the terpenoid pathway after treatment with

[1]International Cooperation Base of Science and Technology Innovation on Forest Resource Biotechnology of Hunan Province, Central South University of Forestry & Technology, Changsha, Hunan, China. [2]Hunan Provincial Key Laboratory of Forestry Biotechnology, Central South University of Forestry & Technology, Changsha, Hunan, China. [3]Yuelushan Laboratory of Seed Industry of Hunan, Changsha, China. ✉e-mail: wxlcsedu@163.com; gaoliuedu@csuft.edu.cn

400 ppm PBZ[19]. However, there are no reports on the application of PBZ to fungi.

In addition to studies on improving triterpenoid production, some studies have revealed the regulatory mechanisms of triterpenoid biosynthesis under chemical inducers in *Sanghuangporus*. To date, studies have focused on altered expression levels of structural genes related to triterpenoid biosynthesis in the MVA pathway, leading to an increase in terpenoid production[12,14]. Nevertheless, the upstream pathways of these known structural genes, especially the transcription factors that regulate their expression, remain poorly understood with respect to the regulatory mechanism of triterpenoid biosynthesis in *Sanghuangporus*.

In this study, the effects of different concentrations of several PGRs on triterpenoid yield and mycelial growth during submerged fermentation of *S. lonicericola* were investigated. Metabolomic and transcriptomic assays were then performed to analyze the composition of triterpenoid compounds and the expression patterns of genes involved in triterpenoid biosynthesis under PBZ treatment. A targeted MYB transcription factor (SlMYB) was further identified using RNA-seq data and bioinformatics analyses. Furthermore, the *SlMYB* gene was manipulated to verify its effect on regulating triterpenoid biosynthesis by constructing mutants, which identified its potential targeted genes. An electrophoretic mobility shift assay (EMSA) was performed to verify the SlMYB protein interactions with promoters of SlMYB targets. Taken together, this study is to apply PBZ to promote triterpenoid biosynthesis and clarify a MYB transcription factor (SlMYB) that responds to PBZ induction and directly regulates triterpenoid biosynthetic genes, including *MVD*, *IDI*, and *FDPS* in *S. lonicericola*.

## Results

### Effects of PGRs on triterpenoid synthesis and mycelial growth

First, four plant growth regulators (PGRs) (PBZ, NAA, IAA, and 6-BA) at different concentrations (0, 10, 50, and 100 mg/L) were added to the fermentation medium to investigate their effects on triterpenoid yield and mycelial growth in *S. lonicericola*. As shown in Fig. 1a, the addition of PBZ and IAA significantly enhanced the triterpenoid yield from 10 to 100 mg/L. The maximum triterpenoid yields of 42.341 ± 0.442 mg/g and 27.864 ± 1.069 mg/g were achieved under 100 mg/L PBZ induction and 50 mg/L IAA induction, respectively, which were 151.39% and 65.43% higher than CK (16.843 ± 0.509 mg/g). Nevertheless, NAA and 6-BA induction had no significant effect on the triterpenoid yield ($P > 0.05$). As shown in Fig. 1b, when the concentration of PBZ was 10 or 50 mg/L, PBZ induction did not affect the biomass ($P > 0.05$). However, the higher concentration (100 mg/L) of PBZ inhibited the mycelial growth of *S. lonicericola*. In addition, biomass increased significantly in the range of 10–100 mg/L of NAA and IAA induction, respectively, and 6-BA induction did not affect biomass ($P > 0.05$). Given the inhibitory action of PBZ on mycelial growth, triterpenoid production was calculated by combining the biomass and triterpenoid yields (Fig. 1c). Induction with NAA and 6-BA did not affect triterpenoid production ($P > 0.05$). Notably, although the biomass under PBZ induction decreased significantly at 100 mg/L, triterpenoid production was significantly higher than that under IAA induction. Moreover, the above parameters showed no significant differences between the Mock and CK (DMSO) groups, indicating that the solvent did not affect triterpenoid yield or mycelial growth of *S. lonicericola* ($P > 0.05$).

IAA and PBZ induction significantly increased the triterpenoid yield of *S. lonicericola*; however, PBZ induction had a greater effect. Therefore, PBZ was considered the optimal inducer with an additional concentration of 100 mg/L for further study.

### Widely targeted metabolomic profiling under PBZ induction

To compare the differences in metabolic levels caused by PBZ induction in *S. lonicericola*, a widely targeted metabolome analysis was performed using an LC-ESI-MS/MS system. The fermented mycelia cultivated for 2 and 4 d under uninduced and PBZ-induced conditions were sampled as the CK2, CK4, PBZ2, and PBZ4 groups, respectively. A total of 801 metabolites were detected, of which 409 and 392 were detected in the positive and negative ion modes, respectively (Supplementary Fig. 1). The PCA results showed an evident separation of metabolic patterns among the four groups (CK2, CK4, PBZ2, and PBZ4) (Supplementary Fig. 2a). The OPLS-DA of the CK2 vs. PBZ2 and CK4 vs. PBZ4 groups were separately clustered into two groups, indicating that PBZ induction changed the metabolite abundance of *S. lonicericola* under submerged fermentation (Supplementary Fig. 2b–c). The integral correction diagrams representing the relative quantification of example metabolites were provided (Supplementary Fig. 3). The abundance of 29 triterpenoids was then illustrated, of which only four decreased. Notably, of the remaining 25 triterpenoids that increased in abundance, 18 were present in the PBZ groups (PBZ2 and PBZ4) and were not detected in the CK groups (CK2 and CK4) (Fig. 2a), suggesting that PBZ induction markedly increased the diversity of triterpenoids in *S. lonicericola*. Subsequently, differential triterpenoid metabolites (DTMs) were screened by OPLS-DA (VIP ≥ 1, $P < 0.05$) among the CK2 vs. PBZ2, CK4 vs. PBZ4, and PBZ2 vs. PBZ4 groups, respectively, aiming to analyze the changes in the composition of triterpenoids. There were four DTMs in the CK2 vs. PBZ2 group: viz. betulin (Compound **17**), 2α-hydroxyursolic acid (**20**), 2α,3α,23-trihydroxyolean-12-en-28-oic acid (**23**), and madasiatic acid (**24**). Compounds **20, 23**, and **24** were absent in CK2 (Fig. 2b). There were eight DTMs in the CK4 vs. PBZ4 group: viz. betulin (Compound **17**), 2α-hydroxyursolic acid (**20**), 2α,3α,23-trihydroxyolean-12-en-28-oic acid (**23**), madasiatic acid (**24**), phytolaccagenin (**25**), alphitolic acid (**26**), 2-hydroxyoleanolic acid (**27**), and maslinic acid (**28**). Besides compound **17**, the other seven DTMs were absent in CK4 (Fig. 2c). There were six DTMs in the PBZ2 vs. PBZ4

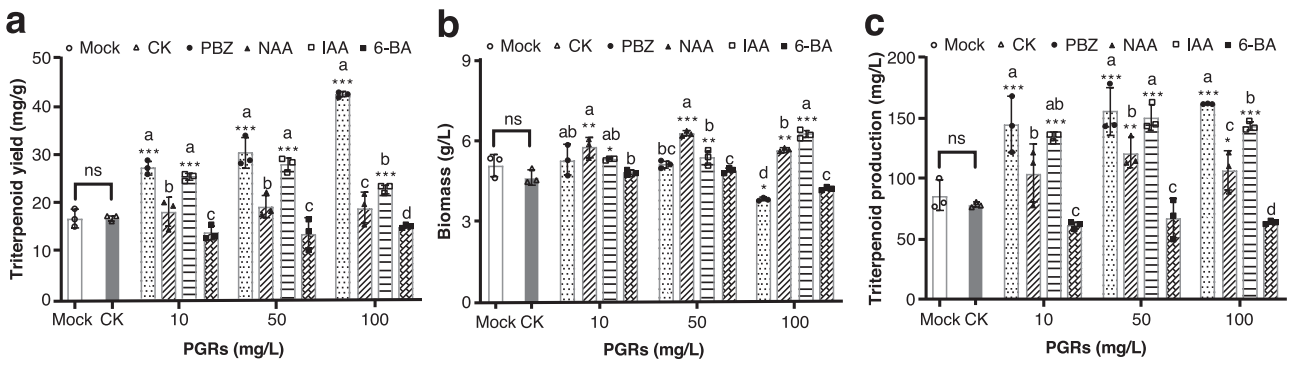


**Fig. 1 | Effects of different PGRs on triterpenoid biosynthesis and mycelial growth at different concentrations under *S. lonicericola* fermentation. a–c** The triterpenoid yield, biomass, and triterpenoid production under PBZ, NAA, IAA, and 6-BA induction. Non-treatment and solvent (DMSO) were used as the Mock and CK, respectively. The values with error bars are the means ± SD ($n = 3$, independent experiments), and the statistical analysis was performed by Duncan's multiple range test. "ns" indicates no statistically significant differences between groups ($P > 0.05$). Different letters indicate significant differences between groups (PBZ, NAA, IAA, and 6-BA) ($P < 0.05$). Asterisks denote significant differences against the CK of the within group: $^{*}P < 0.05$, $^{**}P < 0.01$, and $^{***}P < 0.001$.

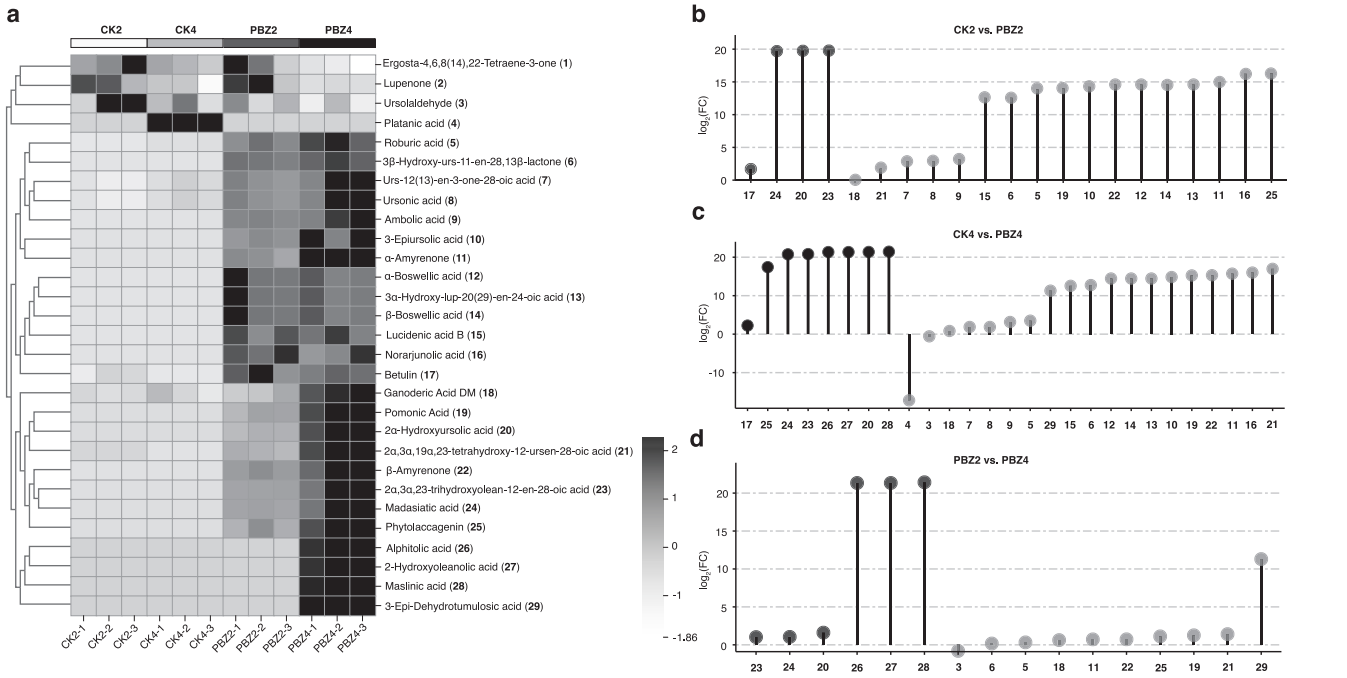


**Fig. 2 | Metabolomic profiling of *S. lonicericola* under PBZ induction. a** Heatmap showing the changes in abundance of detected triterpenoids under PBZ induction. The corresponding triterpenoid compounds are represented by the numbers in parentheses. **b–d** DTMs of CK2 vs. PBZ2, CK4 vs. PBZ4, and PBZ2 vs. PBZ4 groups. DTMs marked in dark lollipops have VIP ≥ 1, *t*-test $P < 0.05$, and $\log_2(FC) > 1$. The remaining compounds are marked in grey lollipops with a *t*-test $P < 0.05$.

group: viz. 2α-hydroxyursolic acid (Compound **20**), 2α,3α,23-trihydroxyolean-12-en-28-oic acid (**23**), madasiatic acid (**24**), alphitolic acid (**26**), 2-hydroxyoleanolic acid (**27**), and maslinic acid (**28**). Compounds **26, 27**, and **28**, were absent in PBZ2, whereas their abundance was significantly increased in PBZ4. The other three DTMs, compounds **20, 23**, and **24**, were detected in PBZ2 and accumulated significantly in PBZ4 (Fig. 2d). In summary, PBZ treatment altered the composition and content of triterpenoids. Among them, the synthesis of some triterpenoids has been enhanced, and the newly generated triterpenoids also contributed to the increase in triterpenoid yield, especially 2α-hydroxyursolic acid (Compound **20**), 2α,3α,23-trihydroxyolean-12-en-28-oic acid (**23**), madasiatic acid (**24**), alphitolic acid (**26**), 2-hydroxyoleanolic acid (**27**), and maslinic acid (**28**). These results showed that PBZ induction led to a significant increase in triterpenoid yield and diversity.

### Transcriptional profiling under PBZ induction

To investigate the differences in mRNA levels caused by PBZ induction, gene expression profiles in *S. lonicericola* were analyzed based on RNA-seq. The distribution of the gene expression levels in the 12 samples is shown in Supplementary Fig. 4a. Three biological replicates of each group clustered together in different areas, revealing that the gene expression patterns changed under PBZ induction. In the comparison groups of CK2 vs. PBZ2 and CK4 vs. PBZ4, 4424 differentially expressed genes (DEGs) (1529 up-regulated and 2895 down-regulated) and 7462 DEGs (1132 up-regulated and 6330 down-regulated) were identified, respectively (Supplementary Fig. 4b). Moreover, 15 key DEGs related to triterpenoid biosynthesis were randomly selected for qRT-PCR validation to further confirm the reliability of the transcriptome data, and the results showed similar expression patterns to those obtained from the RNA-seq data (Supplementary Fig. 5).

To further explore the biological functions of the DEGs induced by PBZ, GO enrichment analysis and KEGG enrichment analysis were performed on the DEGs. 27 and 25 GO terms were significantly enriched in CK2 vs. PBZ2 and CK4 vs. PBZ4 groups, respectively (Fig. 3a–b, Supplementary Fig. 6). Then the shared GO terms at the levels of biological process (BP), molecular function (MF), and cellular component (CC) were analyzed between the two comparison groups (Fig. 3c). Concretely, at the BP level, compared with the CK2 vs. PBZ2 group, significantly enriched GO terms in the CK4 vs. PBZ4 group were significantly increased, suggesting that the metabolic processes were markedly altered with the prolongation of PBZ induction. There were six shared BP terms, including the single-organism process, single-organism metabolic process, isoprenoid metabolic process, acetyl-CoA metabolic process, acyl-CoA metabolic process, and thioester metabolic process. Of these, the three terms including the isoprenoid metabolic process, the acetyl-CoA metabolic process, and the acyl-CoA metabolic process contained the DEGs, such as the hydroxymethylglutaryl-CoA synthase gene (*HMGS*), the hydroxymethylglutaryl-CoA reductase gene (*HMGR*), the diphosphomevalonate decarboxylase gene (*MVD*), and the isopentenyl-diphosphate delta-isomerase gene (*IDI*), that were associated with terpenoid biosynthesis. At the MF level, compared with the CK2 vs. PBZ2 group, significantly enriched GO terms related to "binding" and "oxidoreductase activity" in the CK4 vs. PBZ4 group were significantly decreased and increased, respectively, suggesting that the catalytic reactions were markedly increased to affect the synthesis of metabolites during fermentation. At the CC level, the shared terms were intrinsic component of membrane, membrane part, and membrane. Membranes in filamentous fungi could protect the organism, resist exogenous physical and chemical factors, and participate in metabolic processes[20]. PBZ induction may affect secondary metabolite biosynthesis and metabolism by affecting membrane systems of *S. lonicericola*. Additionally, KEGG enrichment analysis showed the top 25 mapped pathways (Fig. 3d, e). The DEGs were enriched in secondary metabolites, antibiotics, steroids, terpenoid backbone biosynthesis, and amino acid and sugar metabolism. Notably, the terpenoid backbone biosynthesis pathway was significantly enriched in both comparison groups, and the DEGs were mainly involved in the mevalonate pathway (MVA). This suggests that triterpenoids are synthesized through the MVA pathway in *S. lonicericola*, which was in accordance with previous results for *Sanghuangporus sanghuang*, *Sanghuangporus baumii*, and *Sanghuangporus vaninii*[21,22].

### The proposed triterpenoid biosynthetic pathway in *S. lonicericola*

To further explore the mechanism of triterpenoid accumulation under PBZ induction in *S. lonicericola*, the expression patterns of structural genes and

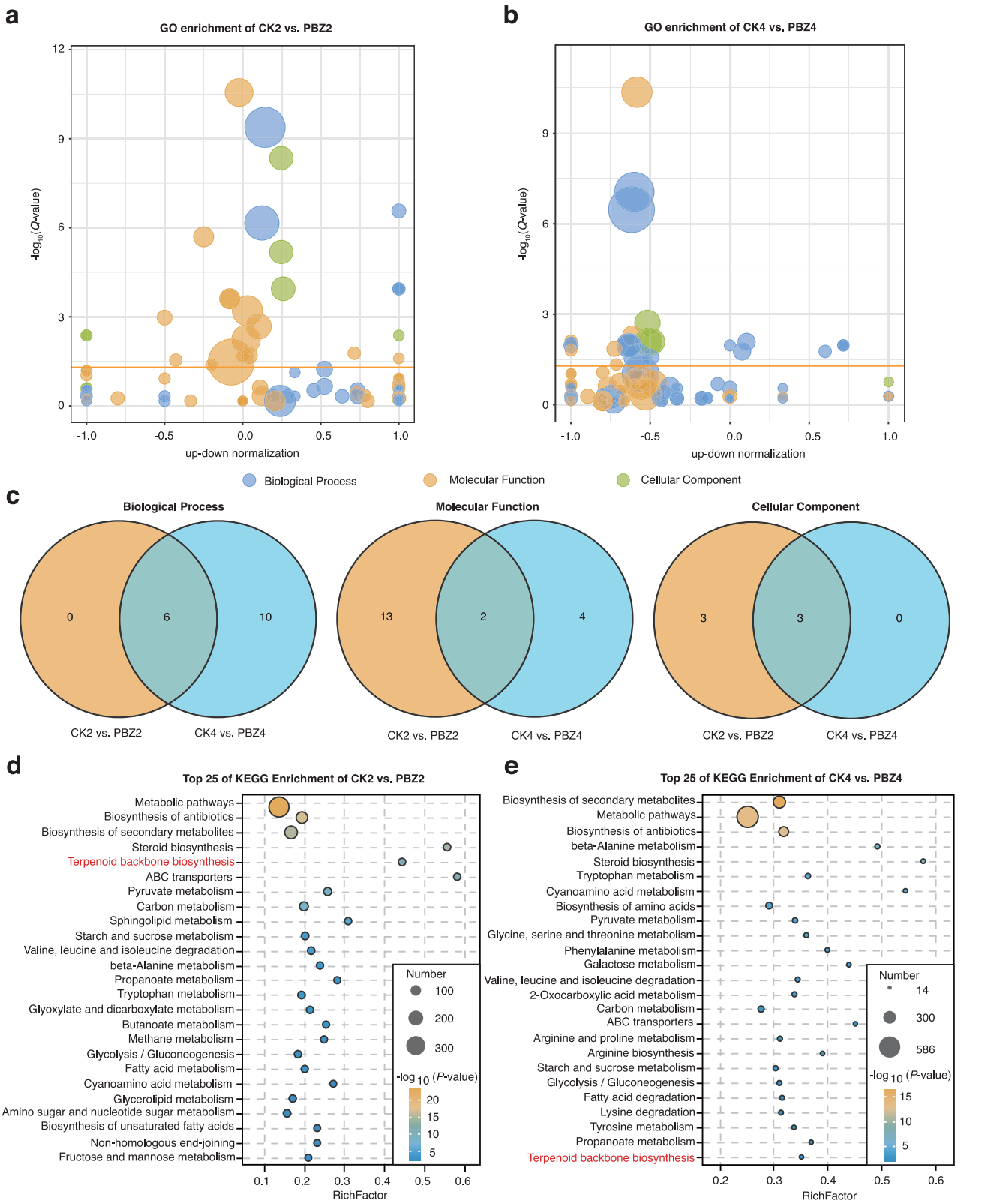


**Fig. 3 | Transcriptional profiling of *S. lonicericola* under PBZ induction. a**, **b** GO enrichment analysis of DEGs of the CK2 vs. PBZ2 and CK4 vs. PBZ4 groups. The yellow line indicates the threshold for *Q*-value = 0.05. **c** Venn diagrams of GO classifications in level 2 between CK2 vs. PBZ2 group and CK4 vs. PBZ4 group. **d**, **e** KEGG enrichment analysis of DEGs of the CK2 vs. PBZ2 and CK4 vs. PBZ4 groups. The terpenoid backbone biosynthesis pathway is marked in red.

metabolites related to triterpenoid biosynthesis were analyzed by integrated omics. 11 enzymes (ACAT, HMGS, HMGR, MVK, PMK, MVD, IDI, FDPS, SQS, SE, and LSS) encoded by 30 genes distributing in the MVA pathway existed in *S. lonicericola*, including three acetyl-CoA C-acetyltransferase genes (*ACAT*), three *HMGS* genes, three *HMGR* genes, two mevalonate kinase genes (*MVK*), two phosphomevalonate kinase genes (*PMK*), five *MVD* genes, two *IDI* genes, three farnesyl diphosphate synthase genes (*FDPS*), two squalene synthase genes (*SQS*), two squalene

monooxygenase genes (*SE*), and three lanosterol synthase genes (*LSS*) (Supplementary Table 1). As previously reported, lanosterol is the key intermediate of triterpenoid biosynthesis in fungi[23,24], followed by decoration via cytochrome P450 monooxygenases (CYPs) to give rise to assorted triterpenoids[25–27]. In this study, a total of 508 genes were annotated as *CYPs* by gene searching (Supplementary Data. 2). 78 unregulated *CYPs* were further screened from the CK2 vs. PBZ2 and CK4 vs. PBZ4 comparison groups. Among them, 35 *CYPs* with complete conserved domain features were clustered into eight superfamilies (Supplementary Fig. 7). Five of them may be involved in triterpenoid biosynthesis in fungi[28,29]. Most of the structural genes in the proposed triterpenoid biosynthesis pathway were highly expressed upon PBZ induction (Fig. 4). Moreover, mevalonic acid (MVA), an intermediate in the MVA pathway, was discovered by shared KEGG pathway analysis (Supplementary Fig. 8), and its abundance was upregulated under PBZ induction (Fig. 4).

### Identification of MYB transcription factors, in response to PBZ induction, that potentially negatively regulate triterpenoid biosynthesis

Chemical inducers alter the expression patterns of many structural genes and regulate terpenoid biosynthesis in *Sanghuangporus*[12,14,30]. However, the regulatory mechanisms of the upstream pathways of these genes under induction remain unknown. Extensive studies have shown that MYB transcription factors (MYB TFs) are involved in regulating terpenoid biosynthesis in plants[31–33]. Because terpenoid biosynthesis in both plants and fungi can be accomplished through the MVA pathway, it was speculated that MYB TFs may regulate triterpenoid biosynthesis in *S. lonicericola*. Additionally, the mechanism of PBZ induction affecting the expression of MYB TFs was preliminarily analyzed.

The transcription factor GlMyb, involved in spermidine biosynthesis and the accumulation of ganoderic acids (GAs) in *Ganoderma lucidum*[34] (GenBank accession number: UOO00978.1), was used to perform a homology BLAST against the *S. lonicericola* genome database. Two genes (*g03192* and *g07425*) encoding MYB TFs were identified as potential MYB orthologs (Supplementary Table 2). The phylogenetic analysis involved the two candidate MYB TFs with seven MYB amino acid sequences from other species, which indicated that g03192, named SlMYB, has high homology to GlMyb (Supplementary Fig. 9a). To further determine the sequence features of SlMYB, a conserved analysis of the MYB domain was conducted and compared with other MYB TFs from fungi and plants, of which PnMYB4, AtMYB4, and MsMYB are the known R2R3-MYB TFs that act as repressors of terpenoid or flavonoid biosynthesis[35–37]. The conservative domain of SlMYB contained five conserved tryptophan residues, which was in accordance with the characteristic features of the known R2R3-MYB proteins (Supplementary Fig. 9b). Moreover, the expression levels of *SlMYB* decreased with increasing PBZ-induced time and were consistent with the transcriptome analysis (Supplementary Fig. 9c,d). The GO function related to "membrane" was significantly altered under PBZ induction (Fig. 3c), which was similar to previous reports of *S. sanghuang*, where fungal elicitors affected the cell membrane and signal transduction pathways[11]. We thus speculated that the changes of membrane systems may affect signal transduction pathways in *S. lonicericola*. Mitogen-activated protein kinase

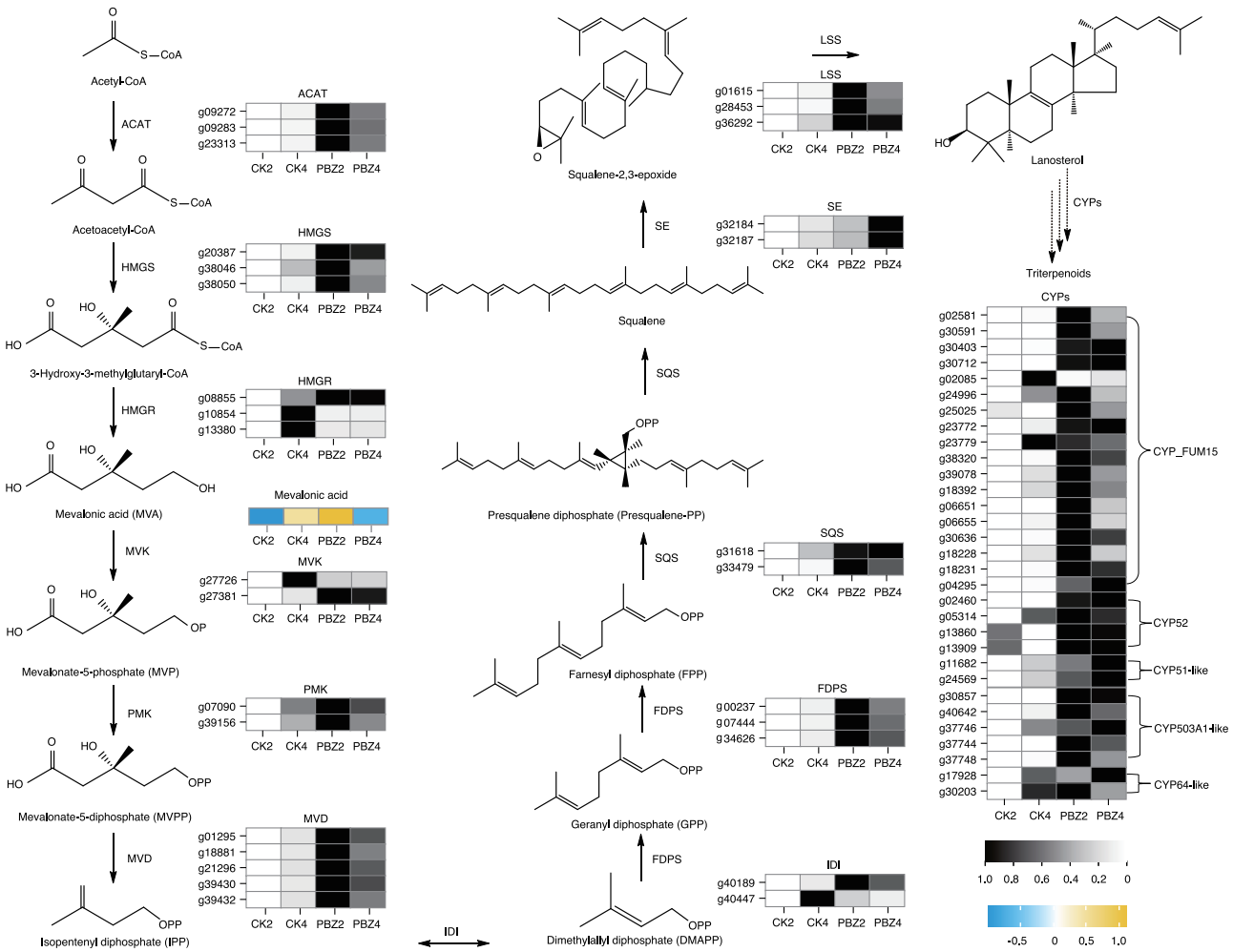


**Fig. 4 | A proposed triterpenoid biosynthesis pathway with the expression profiles of structural DEGs under PBZ induction in *S. lonicericola*.** The dashed line with arrows represents multi-step catalytic reactions.

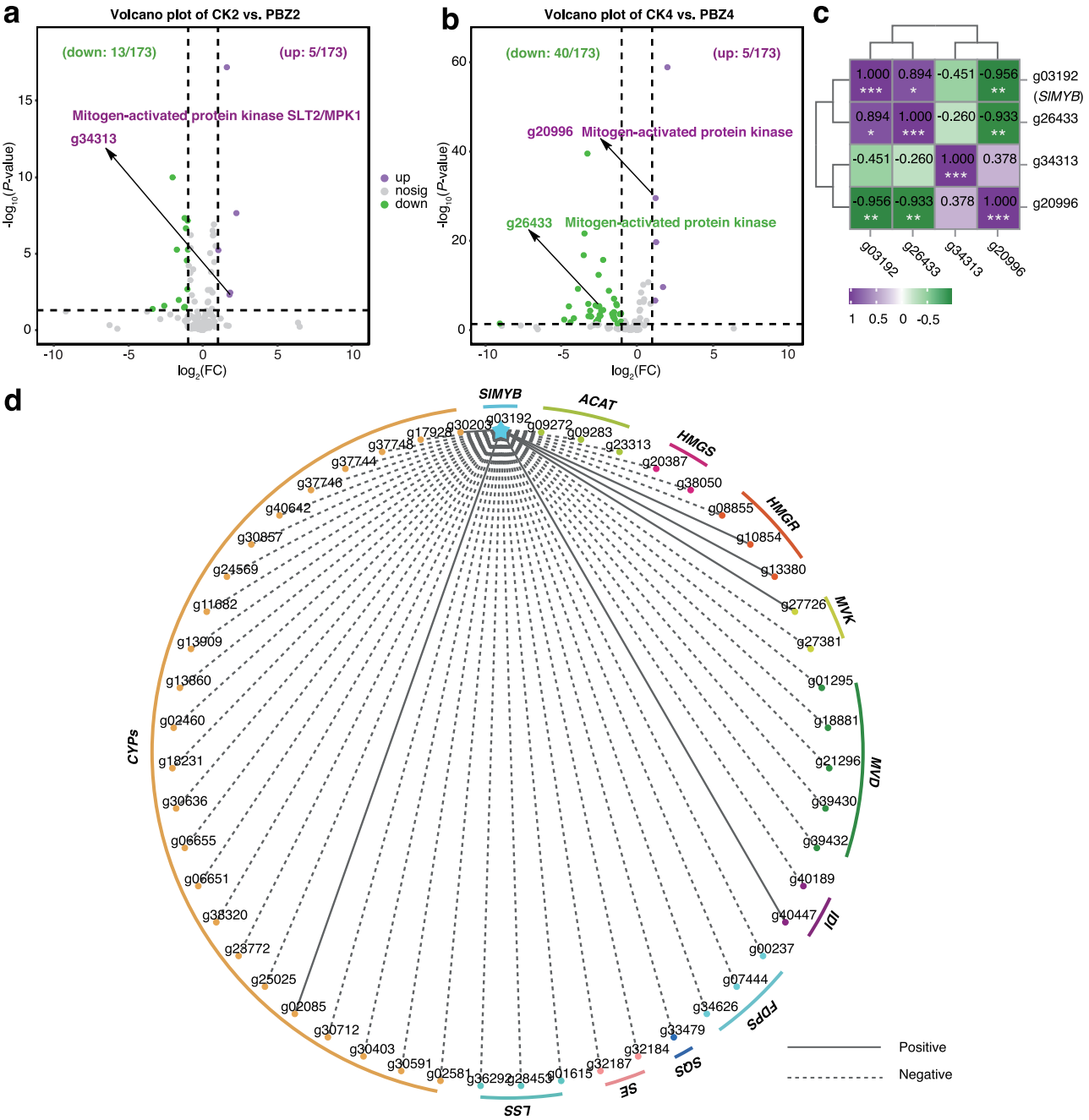


**Fig. 5 | Correlation analysis of SlMYB with MAPKs and structural genes.** Volcano plots of CK2 vs. PBZ2 (**a**) and CK4 vs. PBZ4 (**b**) groups. **c** The correlation analysis of SlMYB and the differentially expressed MAPKs. **d** Correlative network of *SlMYB* and triterpenoid biosynthetic genes, represented by blue star and circles with different colors, respectively. The solid lines and dashed lines represent the positive and negative correlations of relationship pairs according to the absolute Pearson correlation coefficients ≥ 0.8 and $P < 0.05$, respectively.

(MAPK) cascades are conserved signaling pathways in eukaryotes, including fungi, plants, and animals[38]. MAPKs target a wide range of substrate proteins in the nucleus or cytoplasm by phosphorylation, which include other kinases and/or transcription factors[39]. Three differentially expressed MAPKs (*g34313*, *g20996*, and *g26433*) were screened from the CK2 vs. PBZ2 and CK4 vs. PBZ4 comparison groups (Fig. 5a, b), and two of them (*g20996* and *g26433*) were significantly correlated with *SlMYB* (Fig. 5c). These observations indicated that *SlMYB* expression may be regulated by the MAPK signal pathway.

Alternatively, the expression patterns of *SlMYB* were strongly associated with those of the structural genes (Fig. 4), generating a network based on correlation (Fig. 5d). The results showed that *SlMYB* was negatively correlated with the majority of the structural genes, suggesting that SlMYB may be the regulatory repressors of triterpenoid biosynthesis under PBZ induction in *S. lonicericola*.

### RNAi-mediated suppression and overexpression of SlMYB induced triterpenoid biosynthetic gene expression and triterpenoid accumulation in *S. lonicericola*

To clarify the role of *SlMYB* in the regulation of triterpenoid biosynthesis, silenced and overexpression vectors carrying the *Hyg* as screening markers were constructed, respectively (Supplementary Fig. 10). Compared with the WT and CK strains, the transcription levels of *SlMYB* in RNAi-SlMYB-1 and RNAi-SlMYB-2 silenced transformants were significantly decreased by

46% and 59%, respectively, as determined by qRT-PCR (Fig. 6a). The expression levels of *ACAT*, *MVD*, *IDI*, and *FDPS* in silenced strains were markedly increased in comparison to the WT and further increased under PBZ induction (Fig. 6b–e). Notably, the expression levels of *SlMYB* were decreased in comparison to the WT and further markedly decreased under PBZ induction, which was opposite to that of the above structural genes (Fig. 6f). The triterpenoid yield and lanosterol content significantly increased, which was in line with the changes in the patterns of *ACAT*, *MVD*, *IDI*, and *FDPS* (Fig. 6g–h).

Furthermore, the transcription levels of *SlMYB* were significantly increased by 1.86- and 4.41-fold in OE-SlMYB-1 and OE-SlMYB-2 overexpression transformants, respectively (Fig. 6i). In contrast to the results of suppression, overexpression of *SlMYB* inhibited the expression of structural genes (*ACAT*, *MVD*, *IDI*, and *FDPS*) in triterpenoid biosynthesis (Fig. 6j–m). In addition, the expression levels of *SlMYB* increased in comparison to the WT and markedly decreased under PBZ induction compared to the uninduced overexpression transformants (Fig. 6n). The triterpenoid yield and lanosterol content significantly decreased in comparison to the WT and were still higher under PBZ induction than under uninduced conditions (Fig. 6o,p). These results indicated that *SlMYB* is downregulated by PBZ treatment and negatively regulates the expression of *ACAT*, *MVD*, *IDI*, and *FDPS* to promote triterpenoid biosynthesis in *S. lonicericola*.

### SlMYB directly binds to the promoters of *MVD*, *IDI*, and *FDPS*

*MVD*, *IDI*, and *FDPS* were the key triterpenoid biosynthetic genes. Suppression and overexpression of *SlMYB* could significantly increase and decrease the expression of the three genes, respectively. Furthermore, there was one putative MYB binding site (MBS) (CAACAG) within the 2000 bp promoter fragments of *MVD* and *IDI*, respectively, while the 1259 bp promoter contained one MBS (CAACCA) (Supplementary Table. 3). In order to verify the putative MBSs in the promoters of *MVD*, *IDI*, and *FDPS*, the putative DNA binding domain of SlMYB was purified to carry out electrophoretic mobility shift assays (EMSAs). The purified SlMYB domain protein could shift all three DNA fragments, which showed a concentration-dependent trend (Fig. 6q, lines 2-4). The specificity of the SlMYB-DNA complex was confirmed by adding an excess of cold probes. Wakened shifts were detected when adding the cold probes (Fig. 6q, lines 5, 6). These results suggested that SlMYB may play an important role in the triterpenoid accumulation via direct negatively regulation of the transcription of *MVD*, *IDI*, and *FDPS* in *S. lonicericola*.

## Discussion

*Sanghuangporus* fungi are famous and widely used in Asian countries for a long history. More studies have been conducted in several species, including *S. sanghuang*, *S. vaninii*, and *S. baumii*, and found some important bioactive compounds and related biological functions[40–42]. It is also necessary to conduct research on other lesser-attended *Sanghuangporus* species, such as *S. lonicericola*. As major pharmacologically active compounds of *Sanghuangporus* spp., triterpenoid compounds is a hot research topic regarding their yield enhancement by adding elicitors to induce biosynthesis in the culture process. However, the transcription factors that can respond to the induction of elicitors and can directly regulate the expression of triterpenoid biosynthesis genes are still unknown. Here, RNA-seq, metabolomics techniques, and genetic and molecular biology methods, were integrated to clarify the regulatory mechanism of the transcription factor SlMYB in enhancing triterpenoid biosynthesis induced by PBZ in *S. lonicericola*. This study is reported to apply PBZ to promote triterpenoid yield in fungi and to clarify the negative regulatory role of the MYB transcription factor in regulating the expression of target genes related to the triterpenoid biosynthesis by binding their promoter regions.

PGRs are used exogenously as elicitors and exhibit different influences on the growth and biosynthetic pathways of secondary metabolites in plants and fungi. For example, NAA (2.0 mg/L) and 6-BA (1.0 mg/L) could promote oleanolic acid biosynthesis in *Achyranthes bidentata*[43], and NAA (50 mg/L) induction enhanced the shoot length, root length, fresh weight, and dry weight of *Ammi majus*[44]. NAA (20 mg/L) did not affect cell growth but significantly increased flavonoid production in *Phellinus* spp. during fermentation[45]. In the present study, a positive effect of NAA and 6-BA on triterpenoid yield was not observed (Fig. 1a), whereas the effect of NAA induction on mycelial growth was positive (Fig. 1b). Moreover, IAA induction could activate flavonoids, phenols, terpenoids, carbohydrate metabolism, and hormone-signaling pathways to improve kiwifruit resistance[46]. PBZ induction significantly decreased growth parameters, increased the content of terpenoid compounds in *Lavandula officinalis*[19], and promoted sesquiterpene content in *Andrographis paniculata*[47]. Another study showed that PBZ significantly inhibited the elongation of the stipe of *Flammulina filiformis*, a typical agaric fungus[48]. Although the high concentration of PBZ ( ≥ 100 mg/L) significantly inhibited the mycelial growth of *S. lonicericola*, which is consistent with the above evidence, PBZ showed excellent effects on enhancing the triterpenoid biosynthesis compared to the other three PGRs in this study.

18 upregulated triterpenoid compounds were newly generated under PBZ induction, compared to the CK group. Of these, 2α-hydroxyursolic acid, 2α,3α,23-trihydroxyolean-12-en-28-oic acid, madasiatic acid, alphitolic acid, 2-hydroxyoleanolic acid, and maslinic acid were accumulated significantly (Fig. 2). Extensive studies have reported that these compounds possess various pharmacological effects, such as anti-tumor[49], anti-inflammatory[50], hypoglycemic, and anti-parasitic properties[51]. These results indicate that PBZ, as an inducer, could be of great significance in promoting the biosynthesis of triterpenoids with various pharmacological effects in fungi.

The comparative genomics of *S. sanghuang*, *S. baumii*, and *S. vaninii* revealed that the terpenoid backbone biosynthesis involved in triterpenoid biosynthesis is through the conserved MVA pathway[21,22]. Studies showed that the expression patterns of genes in the MVA pathway could be altered in the presence of elicitors to further promote terpenoid biosynthesis. In *S. baumii*, the expression levels of *HMGR*, *IDI*, *SQS*, and *SE* were upregulated under methyl jasmonate (MeJA) treatment[12]. In submerged fermentation with the addition of fungal polysaccharide elicitors, the expression of genes in the terpenoid backbone biosynthesis was significantly upregulated in *S. sanghuang*[11]. In our study, in addition to the majority of genes in terpenoid backbone biosynthesis being highly expressed upon PBZ induction, CYPs classified into different superfamilies were tentatively identified (Fig. 4). According to a recent report, in *Wolfiporia cocos*, *WcCYP_FUM15*, *WcCYP64-1*, and *WcCYP52* have been demonstrated to be involved in catalyzing biosynthetic steps from lanosterol to pachymic acid (PA)[29]. AcCyp51 (sterol 14-α-demethylase) was shown to convert lanostane to ergostane triterpenoids by demethylation in the fruiting body of *Antrodia cinnamomea*[28]. The function of the CYP503A1-like superfamily was similar to the CYP51-like superfamily, according to the annotations in the NCBI database. We thus speculated that the increase of triterpenoid yield and diversity was due to the up-regulation of structural genes induced by PBZ and the multiple catalytic functions, such as oxidation, reduction, methylation, and acetylation, of CYPs in *S. lonicericola*.

The above studies showed that elicitors changed the expression of structural genes. How upstream transcription factors regulate these genes involved in triterpenoid biosynthesis under PBZ induction is worth further study. The mechanisms by which MYB TFs in response to chemical inducers regulate terpenoid biosynthesis in fungi are rarely reported. Although genome-wide comparative annotation analysis showed the MYB genes participating in various biological processes in *Ganoderma*, further function validations are rarely reported[52]. Meanwhile, the functions of MYB TFs in regulating triterpenoid synthesis remain elusive in *Sanghuangporus*. In our study, the expression of *SlMYB* was downregulated by PBZ induction, probably owing to the regulation of MAPK signal pathways (Fig. 5a–c). MAPKs transduce environmental and developmental cues into intracellular responses under numerous processes, including biotic and abiotic stress and hormonal responses[39]. The hormone-responsive transcription factors are subject to multiple post-translational modifications, such as phosphorylation, which can affect protein stability[53]. Although the roles of MYB proteins

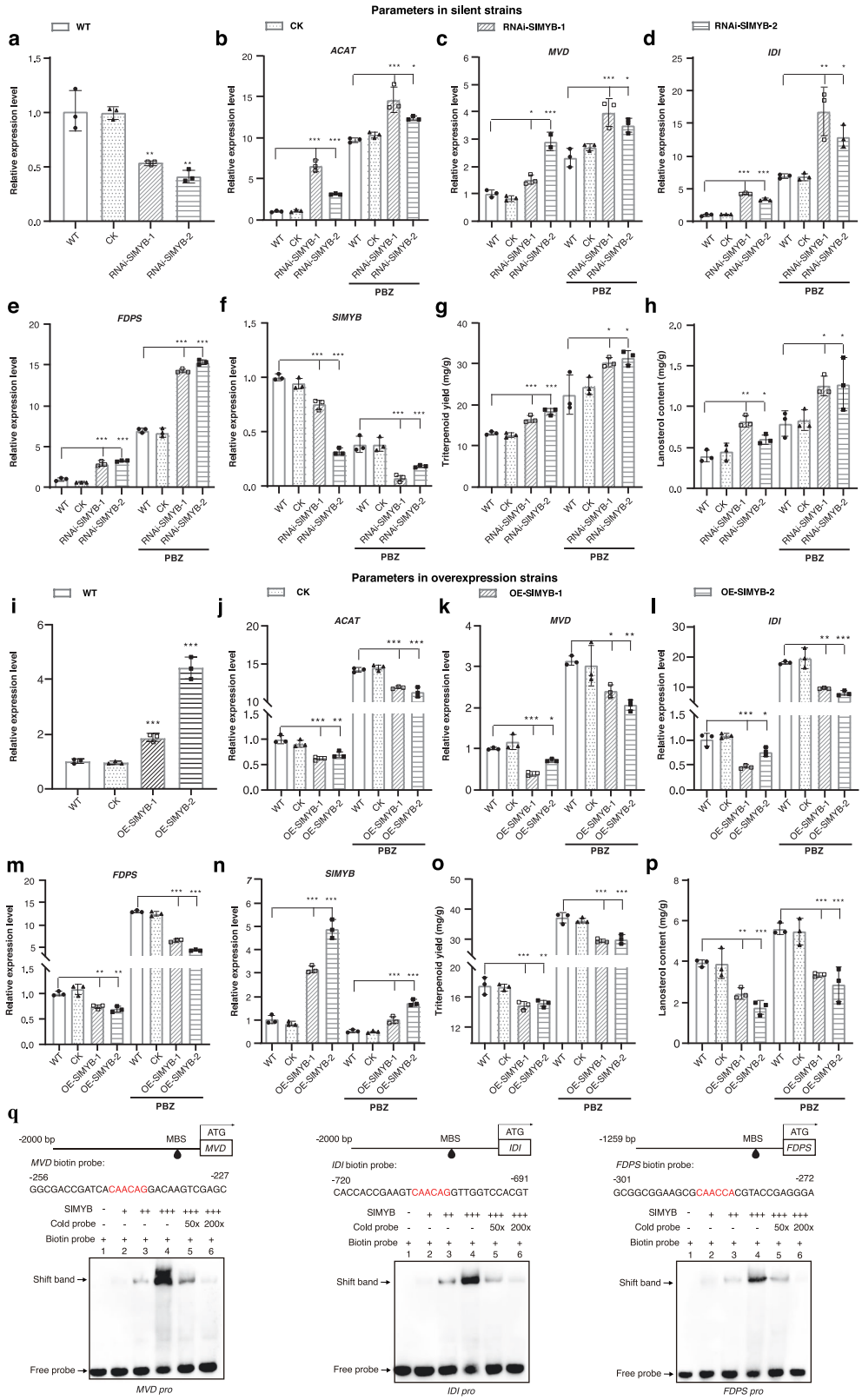


**Fig. 6 | SlMYB regulated triterpenoid biosynthesis in *S. lonicericola*. a-f, i–n.** qRT-PCR analysis of *SlMYB* and four triterpenoid biosynthetic genes in silent or overexpression transformants, respectively. The expression level of each gene in the WT strain was arbitrarily designated as a value of 1 and was normalized with the amount of *UBQ3*. CK represents the empty vector control. **g, h and o, p**. Triterpenoid yield and the lanosterol content in WT, *SlMYB*-silenced strains, and overexpression strains. The values with error bars are the means ± SD ($n = 3$, independent experiments). Asterisks denote significant differences in parameters against the WT: $^{*}P < 0.05$, $^{**}P < 0.01$, $^{***}P < 0.001$, according to Duncan's multiple range test. **q** SlMYB can bind to the DNA sequences in the targets promoter by EMSA. The biotin labeled DNA probe control (Line 1). The biotin-labeled probe was pre-incubated with different concentrations of the purified SlMYB protein (Line 2-4), and the cold probe (50× and 200× biotin-labeled DNA probe) was added (Line 5 and 6).

in fungi remain poorly understood, those in plant growth, development, stress responses, and secondary metabolite production are elucidated and well summarized[54]. In *Arabidopsis*, the phosphorylation of MYB41 and MYB44 by MPKs (MPK3, MPK6) was required for their biological function[55,56]. Another study showed that MPK4 phosphorylation of MYB75 increased its stability and was required for anthocyanin accumulation[57]. Interestingly, MYB44 regulated MPK3 and MPK6 to activate their expression, leading to phosphorylation of MPK3 and MPK6; in turn, phosphorylated MPK3 and MPK6 phosphorylate MYB44, further enabling MYB44 to activate the expression of MPK3 and MPK6[58]. Overexpression of *MaMPK14* and *MaMYB4* delayed fruit ripening in *Musa acuminata* (banana), indicating their negative roles in the ripening. It was found that phosphorylation of MaMYB4 by MaMPK14 enhanced its binding strength, protein stability, and the repression of fruit ripening[59]. The protein abundance of putative transcription factors (including a Myb DNA-binding protein) phosphorylated by *CcPmk1* in *Cytospora chrysosperma* was downregulated in the *CcPmk1* deletion mutant[60]. Collectively, the gene expression and functions of MYB proteins could be regulated by means of phosphorylation via the MAPK signal pathway. We thus speculated that PBZ treatment affected the MAPK signal pathway, leading to phosphorylation of SlMYB protein to further downregulate its expression. Additionally, *SlMYB* was negatively correlated with the expression patterns of most structural genes (Fig. 5d). Genetic manipulation of *SlMYB* suggested that SlMYB acted as a repressor in regulating the transcription of *ACAT*, *MVD*, *IDI*, and *FDPS* involved in triterpenoid biosynthesis in *S. lonicericola* (Fig. 6a–p). MYB TFs always bind to the promoters of target genes to regulate their expression, thereby affecting the production of terpenoid compounds. For example, PnMYB4 could regulate the expression of *PnSS*, *PnSE*, and *PnDS* by combining with the MBSs [(C/T)AAC(T/C)(G/A)] in the promoters of *PnSS*, *PnSE*, and (TAACCA) in the *PnDS* promoter, respectively[36]. In *S. baumii*, the *HGMR* gene promoter contains one putative MBS[12]. Herein, it can be seen that promoter regions of various terpenoid synthetic genes contain MBSs, suggesting triterpenoid biosynthesis could be regulated by MYB TFs. In the present study, the analysis results by using the online PLANTCARE database showed that the promoters of *MVD*, *IDI*, and *FDPS* contained putative MBSs [CAAC(A/C)(G/A)], except the *ACAT*. EMSA experiments suggested that SlMYB can bind to the putative DNA sequence of the promoters of *MVD*, *IDI*, and *FDPS* (Fig. 6q), which provides a reference for studying other target genes in *Sanghuangporus*.

In summary, a more comprehensive mechanism of PBZ-induced biosynthesis of triterpenoids in *S. lonicericola* was proposed: a MYB transcription factor (SlMYB), which was downregulated in response to PBZ induction; SlMYB directly upregulated the expression of *MVD*, *IDI*, and *FDPS*, associated with triterpenoid biosynthesis, which ultimately improved the triterpenoid yield with the increasing diversity of triterpenoid compounds in the edible and medicinal fungus *S. lonicericola* (Fig. 7). This work provides an efficient fermentation strategy to improve triterpenoid synthesis in *Sanghuangporus* species and a potential direction for research on the

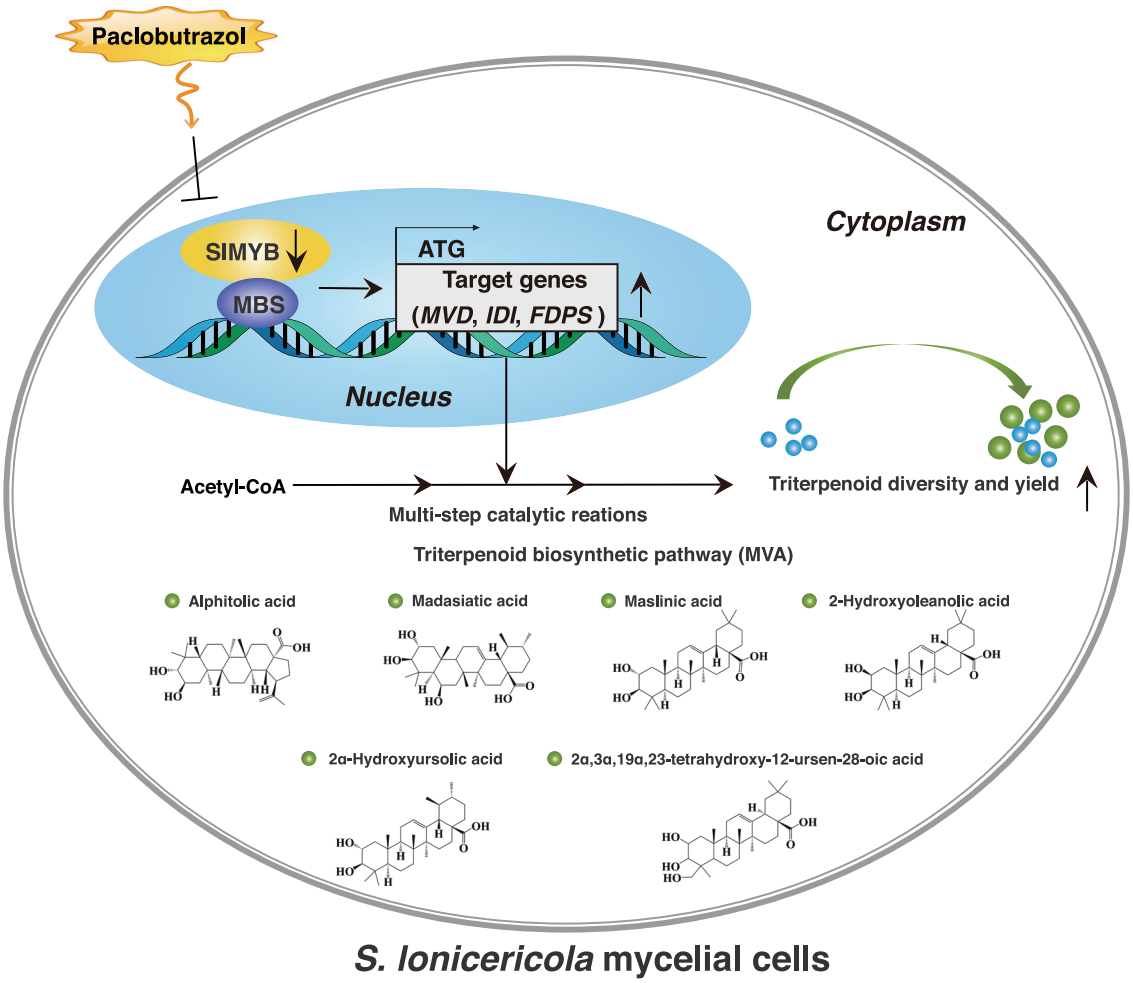


**Fig. 7 | Model depicting the mechanisms of SlMYB in enhancing triterpenoid biosynthesis under PBZ induction in *S. lonicericola*.** The SlMYB transcription factor is downregulated by PBZ induction. SlMYB directly interacts with the promoter regions of *MVD*, *IDI*, and *FDPS*. Downregulated SlMYB promotes the transcription of its target genes that are involved in triterpenoid biosynthesis in the MVA pathway. Triterpenoid yield and diversity increase, and the representative triterpenoid compounds that significantly accumulated are displayed.

regulatory mechanisms of MYB transcription factors in triterpenoid synthesis in fungi. However, future investigation is required to elucidate the detailed underlying mechanism by which PBZ affects the SlMYB transcription factor. At the same time, the transgenic lines of identified *CYPs* should be developed to elucidate their roles in the triterpenoid biosynthetic pathway in *S. lonicericola* in the future.

## Methods

### Microorganisms and culture conditions

*Sanghuangporus lonicericola* strain (Dai 15990), isolated and identified by Professor Dai Yucheng of the Beijing Forestry University, was used in this study. The stock culture was maintained on a potato-dextrose-agar (PDA) medium. The fresh strain was transferred onto a PDA plate to be cultivated at 28 °C for 9–10 days and stored at 4 °C. Subculturing was conducted once a month to maintain the strain activity. The seed medium was composed of the following (in g/L): glucose (20), yeast extract (5), $KH_2PO_4$ (1), and $MgSO_4{\cdot}7H_2O$ (0.5) at a natural pH. The seed culture was obtained at 28 °C and 160 rpm in a rotary shaker for seven days. The basic fermentation medium was composed of the following (in g/L): glucose (20), yeast extract (3), $KH_2PO_4$ (1), and $MgSO_4{\cdot}7H_2O$ (0.5). The pH was adjusted to around 7.0 by progressively adding 1 mol/L HCl or 1 mol/L NaOH. PGRs, including paclobutrazol (PBZ), naphthaleneacetic acid (NAA), indoleacetic acid (IAA), and 6-benzylaminopurine (6-BA), were dissolved in dimethyl sulfoxide (DMSO) to formulate the stock solution, then filtered and sterilized under sterile conditions with 0.22 μm organic syringe filters. The stock solution was slowly added to the sterilized basic fermentation medium before inoculation. Submerged cultivation was performed with 10% (*v*/*v*) of seed stock at 28 °C and 180 r/min for seven days.

### Measurement of mycelial biomass

After cultivation, the fermented mycelia were harvested by 80-mesh sieve filtration and washed thoroughly with distilled water. Afterward, the mycelia were dried at 60 °C overnight to a constant weight. The biomass was determined by the gravimetric method of cell dry weight.

### Determination of intracellular triterpenoid yield and lanosterol content

The dried mycelia were ground to powder using a tissue homogenizer for triterpenoid and lanosterol extraction. For the determination of triterpenoid yield, the mycelia powder (50 mg) was extracted with 90% (*v*/*v*) ethanol (material-to-liquid ratio, 1:50). The sample mixture was heated at 70 °C for 1 h in a thermostat water bath and further extracted by an ultrasonic cleaner at 50 °C for 1 h. The extract mixture was centrifuged at 8000 r/min for 10 min. The supernatant was obtained to determine the triterpenoid yield using a microplate reader (SpectraMax ABS Plus, Molecular Devices, USA). The steps for determination are as follows: Supernatant samples (50–100 μL) were evaporated to dryness with a dry bath (98 °C); 5% vanillin-glacial acetic acid solution (400 μL) and perchloric acid (1 mL) were added sequentially to the dried samples; they were put in a thermostat water bath (60 °C for 15 min) and then cooled down to room temperature; glacial acetic acid (5 mL) was added, mixed well, and left for 20 min; absorbance was measured at 548 nm using ursolic acid as the standard.

For the determination of lanosterol content, the dried mycelia powder (50 mg) was extracted with 10% KOH-75% ethanol (1.5 mL) using a dry bath (50 °C for 2 h) for saponification shaking at 500 r/min. The saponified samples were centrifuged at 12,000 r/min for 10 min. Afterwards, the supernatant was extracted twice with an equal volume of n-hexane. The n-hexane layer was pooled and washed twice with distilled deionized water, and ultimately the solvent was evaporated to dryness. The dry samples were redissolved in 400 μL of acetonitrile and filtered with 0.22 μm organic syringe filters, later injected into a liquid chromatography (SCL-10A, Shimadzu, Japan) equipped with a Symmetry-C18 reversed-phase column (4.6 × 250 mm, 5 μm) detecting at 205 nm. The mobile phase was 100% methanol. Chromatographic peaks of samples were identified by comparison of the retention times and spectra using lanosterol ( ≥ 95%, Aladdin) as the standard.

### Widely targeted metabolomic assays

Samples from the control and PBZ treatment groups were harvested on the second and fourth days, respectively, centrifuged at 5000 r/min for 5 min, and rinsed three times with PBS. The freeze-dried samples were crushed in a mixer mill (MM 400, Retsch) with zirconia beads for 1.5 min at 30 Hz. The powder (100 mg) was extracted overnight at 4 °C with 1 mL of 70% aqueous methanol containing 0.1 mg/L lidocaine as an internal standard. Following centrifugation at 10,000 × *g* for 10 min, the supernatant was absorbed and filtered (SCAA-104, 0.22 μm pore size; ANPEL, Shanghai, China, http://www.anpel.com.cn/) before liquid chromatography–tandem mass spectrometry (LC–MS/MS) analysis. Metabolomic profiling was performed in collaboration with Gene Denovo Biotechnology Co., Ltd. (Guangzhou, China).

Sample extracts were analyzed using an liquid chromatography–electrospray ionization–tandem mass spectrometry (LC–ESI–MS/MS) system (Shim-Pack UFLC SHIMADZU CBM30A system, http://www.shimadzu.com.cn/; MS/MS, Applied Biosystems 6500 Q TRAP, http://www.appliedbiosystems.com.cn/)[61]. The analytical conditions were as follows: UPLC: column, Waters ACQUITY UPLC HSS T3 C18 (2.1 mm × 100 mm, 1.8 μm); solvent system, water (0.04% acetic acid): acetonitrile (0.04% acetic acid); gradient program, 95:5 V/V at 0 min, 5:95 V/V at 11.0 min, 5:95 V/V at 12.0 min, 95:5 V/V at 12.1 min, and 95:5 V/V at 15.0 min; flow rate, 0.40 mL/min; column temperature, 40 °C; and injection volume: 2 μL. The effluent was alternately connected to an ESI–triple quadrupole linear ion trap (Q TRAP)–mass spectrometer (MS).

LIT and triple quadrupole (QQQ) scans were acquired on a Q TRAP–MS, the API 6500 Q TRAP LC–MS/MS System, equipped with an ESI Turbo Ion-Spray interface, operating in positive ion mode, and controlled by the Analyst 1.6.3 software (AB Sciex). The ESI source operation parameters were as follows: ion source, turbo spray; source temperature, 500 °C; ion spray (IS) voltage, 5500 V; ion source gas I (GSI), gas II (GSII), and curtain gas (CUR) at 55, 60, and 25.0 psi, respectively; and collision gas (CAD), high. Instrument tuning and mass calibration were performed with 10 and 100 μmol/L polypropylene glycol solutions in QQQ and LIT modes, respectively. QQQ scans were acquired as MRM experiments, with the collision gas (nitrogen) set to 5 psi. The declustering potential (DP) and collision energy (CE) for individual MRM transitions were done with further DP and CE optimization. A specific set of MRM transitions was monitored for each period according to the metabolites eluted within this period. The m/z range was set between 50 and 1000. Data filtering, peak detection, alignment, and calculations were performed using the Analyst 1.6.1 software.

Differential metabolite analysis: The variable importance for the projection (VIP) score of the Orthogonal Partial Least Squares-Discriminant Analysis (OPLS-DA) model[62] was applied to rank the metabolites that were best distinguished among the groups. The threshold for the VIP was set to 1. Additionally, the t-test was used for univariate analysis to screen for differential metabolites. Those with a $P$ value of $t$-test < 0.05 and VIP ≥ 1 were considered the differential metabolites among groups.

### RNA extraction and RNA-seq

Biological samples for transcriptome analysis were fermented in the same batch as that used for metabolomic assays. Then, the mycelia were frozen immediately using liquid nitrogen and stored at −80 °C. Total RNA was extracted from each sample using a TRIzol reagent kit (Invitrogen, Carlsbad, CA, USA) according to the manufacturer's protocol. RNA quality was determined via RNase-free agarose gel electrophoresis and assessed using an Agilent 2100 Bioanalyzer (Agilent Technologies, Palo Alto, CA, USA). The mRNA was enriched with oligo (dT) beads, fragmented into short fragments, and reverse transcribed into cDNA using the NEBNext Ultra RNA Library Prep Kit for Illumina (NEB 7530, New England Biolabs, Ipswich, MA, USA). The resulting cDNA libraries were sequenced using an Illumina

Novaseq6000 platform (Gene Denovo Biotechnology Co., Ltd., Guangzhou, China).

High-quality clean reads were further filtered from the raw cleans using Fastp (version 0.18.0)[63] and mapped to the reference genome using HISAT 2.2.4[64]. The mapped reads of each sample were assembled using StringTie v1.3.1[65,66] in a reference-based approach. Fragments per kilobase of transcript per million mapped reads (FPKM) were calculated to quantify gene expression abundance and variations in each transcription region using the RSEM software[67]. Differential expression analysis between the control and treatment groups was performed using the DESeq2 software[68] to identify DEGs. The genes with the parameter of false discovery rate (FDR) < 0.05 and an absolute fold change ≥ 2 were set as the threshold.

### Construction of RNA interference (RNAi) and overexpression plasmids and strains

The RNAi and overexpression vectors were derived from the binary expression vector pCAMBIA 1300 T. The empty vectors were modified to drive the expression of the hygromycin B resistance gene (*Hyg*) through the *CaMV 35S* promoter and glyceraldehyde-3-phosphate dehydrogenase (*CmGPD*) gene promoter from *Cordyceps militaris*. Target genes were ligated into empty vectors for silencing and overexpression to obtain recombinant plasmids. Empty and recombinant plasmids were then transformed into *S. lonicericola* strains using a PEG-mediated method. The in-fusion primers used for recombinant vector construction are listed. *Hyg* was amplified using specific primers to verify positive transformants. Detecting the expression of target genes in positive transformants relative to the WT strain by qRT-PCR. All primers used are listed in Supplementary Table 4.

### Real-time quantitative PCR of gene expression

Purified RNA was reverse transcribed to first-strand cDNA with the RT Mix Kit with gDNA Clean for qPCR (AG11728, Accurate Biotechnology) according to the manufacturer's instructions. The primers for the validation of the transcriptome and the gene expression of *ACAT*, *MVD*, *IDI*, and *FDPS* in transformants are listed in Supplementary Table 4. qRT-PCR was conducted with a SYBR Green Premix Pro Taq HS qPCR Kit (AG11718, Accurate Biotechnology) and a QuantStudio3 real-time PCR system (Life Technologies, Singapore). Relative expression levels of genes were calculated according to the $2^{-\Delta\Delta CT}$ method using the housekeeping genes, *GPD* and *UBQ3*, for reference.

### Electrophoretic mobility shift assay (EMSA)

The coding sequence of the conserved domain of SlMYB was amplified and recombined into the pGEX4T-1 vector (GST-tag) to generate GST infusion protein. In parallel, the 30-nt probes of the promoter containing the putative MYB binding sites of *MVD*, *IDI*, and *FDPS*, were synthesized and biotin labeled at the 5′ end. Cold probes were subjected to competition experiments. EMSA was performed using the Lightshift$^{R}$ Chemiluminescent EMSA Kit (20148, Thermo Scientific) according to the manufacturer's instructions. The biotin signals were imaged using the Chemiluminescence/Fluorescence Imaging System (Tanon-5200Multi, Shanghai, China).

### Statistics and reproducibility

All the data presented in the manuscript are from at least three independent experiments. Error bars indicate standard deviations (SD) from the mean of triplicate independent experiments. Statistical analysis was performed by Duncan's multiple range test and one-way analysis of variance (ANOVA) using SPSS 26. Different letters indicate significant differences between the comparison groups ($P < 0.05$). Single, double, and triple asterisks indicate the significant difference level at $P < 0.05$, $P < 0.01$, and $P < 0.001$, respectively.

### Reporting summary

Further information on research design is available in the Nature Portfolio Reporting Summary linked to this article.

## Data availability

All data generated or analyzed during this study are included in the manuscript and its Supplementary Information files. The Supplementary Figs., tables, and uncropped EMSAs (Supplementary Fig. 11) are available in Supplementary Information. The functional annotations of CYPs are shown in Supplementary Data 1. The source data underlying the graphs in the figure are shown in Supplementary Data 2. The total ion chromatograms (TICs) of each sample are provided in Supplementary Data 3. The mapping table for detected metabolites is provided in Supplementary Data 4. The reference genome data of RNA-seq in this paper is associated with NCBI BioProject: PRJNA587366 and BioSample: SAMN13189427. The raw RNA-seq data are not available because the downloadable period provided by the company analyzing the data has expired, resulting in the data being deleted and no backup being available. The processed RNA-seq data are provided in Supplementary Data 5.

Received: 25 October 2024; Accepted: 24 March 2025;
Published online: 03 April 2025

## References

1. Zhou, L.W. et al. Global diversity and taxonomy of the *Inonotus linteus* complex (Hymenochaetales, Basidiomycota): *Sanghuangporus* gen. Nov., *Tropicoporus excentrodendri* and *T. guanacastensis* gen. et spp. Nov., and 17 new combinations. *Fungal Divers.* **77**, 335–347 (2016).
2. Wu, F., Qin, W.M., Euatrakool, O. & Zhou, L.W. *Tropicoporus boehmeriae* sp. Nov. (Hymenochaetaceae, Basidiomycota) from Thailand, a new member of the *Inonotus linteus* complex. *Phytotaxa* **231**, 73–80 (2015).
3. Zhu, L., Xing, J.H. & Cui, B.K. Morphological characters and phylogenetic analysis reveal a new species of *Sanghuangporus* from China. *Phytotaxa* **311**, 270–276 (2017).
4. Wu, S.H., Chang, C.C., Wei, C.L., Jiang, G.Z. & Cui, B.K. *Sanghuangporus toxicodendri* sp. Nov. (Hymenochaetales, Basidiomycota) from China. *Mycokeys* **57**, 101–111 (2019).
5. Wu, F., Zhou, L.W., Vlasak, J. & Dai, Y.C. Global diversity and systematics of Hymenochaetaceae with poroid hymenophore. *Fungal Divers.* **113**, 1–192 (2022).
6. Zhou, L.W., Ghobad-Nejhad, M., Tian, X.M., Wang, Y.F. & Wu, F. Current status of 'Sanghuang' as a group of medicinal mushrooms and their perspective in industry development. *Food Rev. Int.* **38**, 589–607 (2022).
7. Lu, J.G. et al. Research progress of bioactive components in *Sanghuangporus* spp. *Molecules* **29**, 1195 (2024).
8. Cai, C.S. et al. Extraction and antioxidant activity of total triterpenoids in the mycelium of a medicinal fungus, *Sanghuangporus sanghuang*. *Sci. Rep.* **9**, 7418 (2019).
9. Ma, J.X. et al. In vitro antibacterial and antitumor activity of total triterpenoids from a medicinal mushroom *Sanghuangporus sanghuang* (*Agaricomycetes*) in liquid fermentation culture. *Int. J. Med. Mushrooms* **23**, 27–39 (2021).
10. Huang, J. et al. Unsaturated fatty acid promotes the production of triterpenoids in submerged fermentation of *Sanghuangporus baumii*. *Food Biosci.* **37**, 100712 (2020).
11. Zhou, L.J. et al. Transcriptome and metabolome integration reveals the impact of fungal elicitors on triterpene accumulation in *Sanghuangporus sanghuang*. *J. Fungi* **9**, 604 (2023).
12. Liu, Z.C., Liu, R.P., Tong, X.Y. & Zou, L. New insights into methyl jasmonate regulation of triterpenoid biosynthesis in medicinal fungal species *Sanghuangporus baumii* (Pilat) L.W. Zhou & Y.C. Dai. *J. Fungi* **8**, 889 (2022).
13. Zhou, J. et al. Effects of compound elicitors on the biosynthesis of triterpenoids and activity of defense enzymes from *Inonotus hispidus* (Basidiomycetes). *Molecules* **27**, 2618 (2022).

14. Wang, X.T., Sun, J., Wang, S.X., Sun, T.T. & Zou, L. Salicylic acid promotes terpenoid synthesis in the fungi *Sanghuangporus baumii*. *Microb. Biotechnol.* **16**, 1360–1372 (2023).
15. Assaf, M., Korkmaz, A., Karaman, Ş & Kulak, M. Effect of plant growth regulators and salt stress on secondary metabolite composition in *Lamiaceae* species. *S. Afr. J. Bot.* **144**, 480–493 (2022).
16. Guo, X.B., Wang, L.Z., Chang, X.X., Li, Q. & Abbasi, A.M. Influence of plant growth regulators on key-coding genes expression associated with phytochemicals biosynthesis and antioxidant activity in soybean (*Glycine max* (L.) Merr) sprouts. *Int. J. Food Sci. Technol.* **54**, 771–779 (2018).
17. Desta, B. & Amare, G. Paclobutrazol as a plant growth regulator. *Chem. Biol. Technol. Agric*. **8** (2021).
18. Valdevite, M. et al. Modulation of quinonemethide triterpenes biosynthesis in *Monteverdia floribunda* (Reissek) biral root cultures by exogenous inhibitors. *Plant Cell Tiss. Org.* **149**, 313–324 (2022).
19. El-Sayed, S.M. et al. Exogenous paclobutrazol reinforces the antioxidant and antimicrobial properties of lavender (*Lavandula officinalis* L.) oil through modulating its composition of oxygenated terpenes. *Plants* **11**, 1607 (2022).
20. Higuchi, Y. Membrane traffic related to endosome dynamics and protein secretion in filamentous fungi. *Biosci. Biotechnol. Biochem.* **85**, 1038–1045 (2021).
21. Jiang, J.H., Wu, S.H. & Zhou, L.W. The first whole genome sequencing of *Sanghuangporus sanghuang* provides insights into its medicinal application and evolution. *J. Fungi* **7**, 787 (2021).
22. Shen, Z.Q., Jiang, J.H., Li, C.T., Li, Y. & Zhou, L.W. Genome re-annotation and transcriptome analyses of *Sanghuangporus sanghuang*. *J. Fungi* **9**, 505 (2023).
23. Ríos, J.L., Andújar, I., Recio, M.C. & Giner, R.M. Lanostanoids from fungi: a group of potential anticancer compounds. *J. Nat. Prod.* **75**, 2016–2044 (2012).
24. Wang, Q. et al. Biosynthesis and regulation of terpenoids from basidiomycetes: exploration of new research. *AMB Express* **11**, 150 (2021).
25. Dinday, S. & Ghosh, S. Recent advances in triterpenoid pathway elucidation and engineering. *Biotechnol. Adv.* **68**, 108214 (2023).
26. Li, Y.L. et al. Natural products of pentacyclic triterpenoids: from discovery to heterologous biosynthesis. *Nat. Prod. Rep.* **40**, 1303–1353 (2023).
27. Yuan, W. et al. Biosynthesis of mushroom-derived type II ganoderic acids by engineered yeast. *Nat. Commun.* **13**, 7740 (2022).
28. Lu, M.Y.J. et al. Genomic and transcriptomic analyses of the medicinal fungus *Antrodia cinnamomea* for its metabolite biosynthesis and sexual development. *PNAS* **111**, 15591–15596 (2014).
29. Liu, H.P. et al. An omics-based characterization of *Wolfiporia cocos* reveals three CYP450 members involved in the biosynthetic pathway of pachymic acid. *Commun. Biol.* **7**, 666 (2024).
30. Huang, J. et al. The mechanistic study of adding polyunsaturated fatty acid to promote triterpenoids production in submerged fermentation of *Sanghuangporus baumii*. *Biochem. Eng. J.* **191**, 108800 (2023).
31. Anwar, M., Wang, J.K., Li, J.C., Altaf, M.M. & Hu, Z.L. MYB transcriptional factors affects upstream and downstream MEP pathway and triterpenoid biosynthesis in *Chlamydomonas reinhardtii*. *Processes* **12**, 487 (2024).
32. Sharma, L., Maurya, B., Pandey, S., Rai, K.K. & Pandey-Rai, S. Structural and functional prediction of WsMYB34 transcription factor in *Withania somnifera* (L.) Dunal by deciphering its role in NaCl-induced secondary metabolism. *Ind. Crops Prod.* **206**, 117682 (2023).
33. Yang, Z.Z. et al. MYB21 interacts with MYC2 to control the expression of terpene synthase genes in flowers of *Freesia hybrida* and *Arabidopsis thaliana*. *J. Exp. Bot.* **71**, 4140–4158 (2020).
34. Han, X.F. et al. Phospholipase D and phosphatidic acid mediate regulation in the biosynthesis of spermidine and ganoderic acids by activating GlMyb in *Ganoderma lucidum* under heat stress. *Environ. Microbiol.* **24**, 5345–5361 (2022).
35. Reddy, V.A. et al. Spearmint R2R3-MYB transcription factor MsMYB negatively regulates monoterpene production and suppresses the expression of geranyl diphosphate synthase large subunit (*MsGPPS.LSU*). *Plant Biotechnol. J.* **15**, 1105–1119 (2017).
36. Man, J.H. et al. PnMYB4 negatively modulates saponin biosynthesis in *Panax notoginseng* through interplay with PnMYB1. *Hortic. Res.* **10**, uhad134 (2023).
37. Wang, X.C. et al. *Arabidopsis* MYB4 plays dual roles in flavonoid biosynthesis. *Plant J.* **101**, 637–652 (2019).
38. Colcombet, J. & Hirt, H. *Arabidopsis* MAPKs: a complex signalling network involved in multiple biological processes. *Biochem. J.* **413**, 217–226 (2008).
39. Cristina, M., Petersen, M. & Mundy, J. Mitogen-activated protein kinase signaling in plants. *Annu. Rev. Plant Biol.* **61**, 621–649 (2010).
40. Chien, L.H. et al. Study on the potential of *Sanghuangporus sanghuang* and its components as COVID-19 spike protein receptor binding domain inhibitors. *Biomed. Pharmacother.* **153**, 113434 (2022).
41. Guo, S.S. et al. Component analysis and anti-colorectal cancer mechanism via AKT/mTOR signalling pathway of *Sanghuangporus vaninii* extracts. *Molecules* **27**, 1153 (2022).
42. Yi, Y.J., Lee, I.K., Lee, S.M. & Yun, B.S. An antioxidant davallialactone from *Phellinus baumii* enhances sperm penetration on in vitro fertilization of pigs. *Mycobiology* **44**, 54–57 (2016).
43. Liu, Y.Q., Tang, L., Wang, C. & Li, J.T. NAA and 6-BA promote accumulation of oleanolic acid by JA regulation in *Achyranthes bidentata* Bl. *PLoS One* **15**, (2020). e0229490.
44. Uddin, M. et al. Effect of GA3 and NAA on growth, physiological parameters, and bioactive constituents of *Ammi majus*. *L. Ind. Crops Prod.* **194**, 116328 (2023).
45. Ma, X.K., Li, L., Peterson, E.C., Ruan, T. & Duan, X. The influence of naphthaleneacetic acid (NAA) and coumarin on flavonoid production by fungus *Phellinus* sp.: modeling of production kinetic profiles. *Appl. Microbiol. Biotechnol.* **99**, 9417–9426 (2015).
46. Li, Z.X. et al. Widely targeted metabolomics analysis reveals the effect of exogenous auxin on postharvest resistance to *Botrytis cinerea* in kiwifruit (*Actinidia chinensis* L.). *Postharvest Biol. Technol.* **195**, 112129 (2023).
47. Supaibulwatana, K. et al. Metabolic disturbance and phytochemical changes in *Andrographis paniculata* and possible action mode of andrographolide. *Asian Pac. J. Trop. Biomed.* **8**, 85–91 (2018).
48. Li, H. et al. Targeted metabolome and transcriptome analyses reveal changes in gibberellin and related cell wall-acting enzyme-encoding genes during stipe elongation in *Flammulina filiformis*. *Front. Microbiol.* **14**, 1195709 (2023).
49. Jiang, X., Li, T. & Liu, R.H. 2α-hydroxyursolic acid inhibited cell proliferation and induced apoptosis in MDA-MB-231 human breast cancer cells through the p38/MAPK signal transduction pathway. *J. Agric. Food Chem.* **64**, 1806–1816 (2016).
50. Pan, F.X. et al. Triterpenoids in jujube: a review of composition, content diversity, pharmacological effects, synthetic pathway, and variation during domestication. *Plants* **12**, 1501 (2023).
51. Yan, R. et al. Bioactivities and structure-activity relationships of maslinic acid derivatives: a review. *Chem. Biodivers.* **21**, e202301327 (2024).
52. Wang, L. et al. Genome-wide characterization and comparative analysis of MYB transcription factors in *Ganoderma* species. *G3-GENES Genom. Genet* **10**, 2653–2660 (2020).
53. Hill, K. Post-translational modifications of hormone-responsive transcription factors: the next level of regulation. *J. Exp. Bot.* **66**, 4933–4945 (2015).
54. Bhatt, P.A., Gurav, T.P., Kondhare, K.R. & Giri, A.P. MYB proteins: versatile regulators of plant development, stress responses, and secondary metabolite biosynthetic pathways. *Int. J. Biol. Macromol.* **288**, 138588 (2025).

55. Hoang, M.H.T. et al. Phosphorylation by AtMPK6 is required for the biological function of AtMYB41 in *Arabidopsis*. *Biochem. Biophys. Res. Commun.* **422**, 181–186 (2012).
56. Nguyen, X.C. et al. Phosphorylation of the transcriptional regulator MYB44 by mitogen activated protein kinase regulates *Arabidopsis* seed germination. *Biochem. Biophys. Res. Commun.* **423**, 703–708 (2012).
57. Li, S. et al. MYB75 phosphorylation by MPK4 is required for light-induced anthocyanin accumulation in *Arabidopsis*. *Plant Cell* **28**, 2866–2883 (2016).
58. Wang, Z. et al. MYB44 regulates PTI by promoting the expression of EIN2 and MPK3/6 in *Arabidopsis*. *Plant Commun.* **4**, 100628 (2023).
59. Yang, Y. et al. Mitogen-activated protein kinase 14-mediated phosphorylation of MaMYB4 negatively regulates banana fruit ripening. *Hortic. Res.* **10**, uhac243 (2023).
60. Yu, L., Yang, Y.C., Xiong, D.G. & Tian, C.M. Phosphoproteomic and metabolomic profiling uncovers the roles of CcPmk1 in the pathogenicity of *Cytospora chrysosperma*. *Microbiol. Spectr.* **10**, (2022). e0017622.
61. Chen, W. et al. A novel integrated method for large-scale detection, identification, and quantification of widely targeted metabolites: application in the study of rice metabolomics. *Mol. Plant* **6**, 1769–1780 (2013).
62. Worley, B. & Powers, R. Multivariate analysis in metabolomics. *Curr. Metabolomics* **1**, 92–107 (2012).
63. Chen, S.F., Zhou, Y.Q., Chen, Y.R. & Gu, J. Fastp: an ultra-fast all-in-one FASTQ preprocessor. *Bioinf* **34**, i884–i890 (2018).
64. Kim, D., Langmead, B. & Salzberg, S.L. Hisat: a fast spliced aligner with low memory requirements. *Nat. Methods* **12**, 357–360 (2015).
65. Robinson, M.D., McCarthy, D.J. & Smyth, G.K. EdgeR: a bioconductor package for differential expression analysis of digital gene expression data. *Bioinf* **26**, 139–140 (2010).
66. Pertea, M. et al. Stringtie enables improved reconstruction of a transcriptome from RNA-seq reads. *Nat. Biotechnol.* **33**, 290–295 (2015).
67. Li, B. & Dewey, C.N. RSEM: accurate transcript quantification from RNA-seq data with or without a reference genome. *BMC Bioinform.* **12**, 323 (2011).
68. Love, M.I., Huber, W. & Anders, S. Moderated estimation of fold change and dispersion for RNA-seq data with DESeq2. *Genome Biol.* **15**, 550 (2014).


## Acknowledgements

This work was supported by the financial support from the National Natural Scientific Foundation of China (32071673), the Program of Hunan Science and Technology Innovation Team (2021RC4063), the Key Scientific Research Project of Hunan Provincial Department of Education (23A0229) and Postgraduate Scientific Research Innovation Project of Hunan Province (CX20220696).

## Author contributions

Dong-Xue Zhang designed the study, carried out experiments, analyzed data, and wrote the manuscript. Bi-Yang Liu, Fei-Fei Xue, and Yu-Lin Tang carried out experiments and analyzed data. Meng-Jiao Yan, Si-Xian Wang, Lu Guo, and Li-Nan Wan contributed to data curation. Tian Tong and Yong-Nan Liu discussed the results. Xiao-Ling Wang designed the study and contributed to conceptualization. Gao-Qiang Liu contributed to overall supervision, reviewing and editing the manuscript. All authors gave input and approved the manuscript.

## Competing interests

The authors declare no competing interests.

## Additional information

**Supplementary information** The online version contains supplementary material available at https://doi.org/10.1038/s42003-025-07987-z.

**Correspondence** and requests for materials should be addressed to Xiao-Ling Wang or Gao-Qiang Liu.

**Peer review information** *Communications Biology* thanks Svetlana Kalinina and the other, anonymous, reviewer for their contribution to the peer review of this work. Primary Handling Editors: Heejin Yoo and Tobias Goris. A peer review file is available.

**Reprints and permissions information** is available at http://www.nature.com/reprints

**Publisher's note** Springer Nature remains neutral with regard to jurisdictional claims in published maps and institutional affiliations.

**Open Access** This article is licensed under a Creative Commons Attribution-NonCommercial-NoDerivatives 4.0 International License, which permits any non-commercial use, sharing, distribution and reproduction in any medium or format, as long as you give appropriate credit to the original author(s) and the source, provide a link to the Creative Commons licence, and indicate if you modified the licensed material. You do not have permission under this licence to share adapted material derived from this article or parts of it. The images or other third party material in this article are included in the article's Creative Commons licence, unless indicated otherwise in a credit line to the material. If material is not included in the article's Creative Commons licence and your intended use is not permitted by statutory regulation or exceeds the permitted use, you will need to obtain permission directly from the copyright holder. To view a copy of this licence, visit http://creativecommons.org/licenses/by-nc-nd/4.0/.

© The Author(s) 2025